Inorg. Chem. **2005**, *44*, 1282–1289

Iridium Cyclometalated Complexes with Axial Symmetry: Time-Dependent Density Functional Theory Investigation of *trans*-Bis-Cyclometalated Complexes Containing the Tridentate Ligand 2,6-Diphenylpyridine

Matthew Polson,*,† Marcella Ravaglia,† Sandro Fracasso,† Marco Garavelli,‡ and Franco Scandola*,†

Dipartimento di Chimica, Università di Ferrara, INSTM, UdR Ferrara, 44100 Ferrara, Italy, and Dipartimento di Chimica "G. Ciamician", 40126 Bologna, Italy

Received June 3, 2004

A new series of iridium cyclometalated complexes with a C∧N∧C dppy-type ligand and a N∧N∧N tpy-type ligand have been synthesized and characterized by various techniques such as mass spectrometry, ^{1}H and ^{13}C NMR, cyclic voltammetry, both steady-state and time-resolved emission and absorption studies, and time-dependent DFT (TDDFT) calculations. The complexes exhibit strong visible absorptions and long-lived (1.6–2.0 μs) emissions (λ_{max}, ca. 680 nm) in room-temperature solution. DFT calculations on the ground-state geometry match that of an X-ray crystal structure. TDDFT calculations give accurate predictions of the electronic absorption energies and intensities, while geometry optimizations on the lowest energy triplet state give accurate energies for the emission. Examination of the relevant molecular orbitals shows that the inherent asymmetry of the coordination environment offers a unique directional character to the emitting excited state, which is predominately LLCT (dppy → tpy) in nature.

Introduction

Polypyridine complexes of d^6 transition metals have been widely studied, because of their useful spectroscopic and photophysical properties. The major role in the field has been played by complexes of divalent metals, such as Ru(II) and Os(II), both as mononuclear and as polynuclear species.[1] In recent years, interest has also been devoted to trivalent metals, especially when complexed by cyclometalating ligands. In particular, Ir(III) cyclometalated complexes have attracted a great deal of attention because of their possible appplications (photonic devices,[2−4] LED displays,[5] electron-transfer sensitizers,[6] photocatalysts for CO_2 reduction,[7] photooxidants or singlet oxygen sensitizers,[8] and labeling reagents for biological substrates[9]).

We have recently reported on a new moiety in Ir(III) polypyridyl chemistry.[10] This iridium complex involves two tridentate ligands: a N∧N∧N-bonded tpy derivative (tpy =

* Authors to whom correspondence should be addressed. E-mail: snf@unife.it (F.S.).
† Università di Ferrara.
‡ Dipartimento di Chimica "G. Ciamician".

(1) (a) Scandola, F.; Chiorboli, C.; Indelli, M. T.; Rampi, M. A. In *Electron Transfer in Chemistry*; Balzani, V., Ed.; Wiley-VCH: Weinheim, Germany, 2001; Vol. III, Chapter 2.3, pp 337−408. (b) Campagna, S.; Serroni, S.; Puntoriero, F.; Di Pietro, C.; Ricevuto, V. In *Electron Transfer in Chemistry*; Balzani, V., Ed.; Wiley-VCH: Weinheim, Germany, 2001; Vol. V, Chapter 1.6, pp 186−214. (c) De Cola, L.; Belser, P. In *Electron Transfer in Chemistry*; Balzani, V., Ed.; Wiley-VCH: Weinheim, Germany, 2001; Vol. V, Chapter 1.3, pp 97−136.
(2) Tamayo, A, B.; Alleyne, B. D.; Djurovich, P. I.; Lamansky, S.; Tsyba, I.; Ho, N. N.; Bu, R.; Thompson, M. E. *J. Am. Chem. Soc*. **2003**, *125*, 7377.
(3) Baldo, M. A.; Thompson, M. E.; Forrest, S. R. *Nature* **2000**, *403*, 750.
(4) Lamansky, S.; Djurovich, P.; Murphy, D.; Abdel-Razzaq, F.; Lee, H.-E.; Adachi, C.; Burrows, P. E.; Forrest, S. R.; Thompson, M. E. *J. Am. Chem. Soc.* **2001**, *123*, 4304−4312.
(5) Nazeeruddin, Md. K.; Humphry-Baker, R.; Berner, D.; Rivier, S.; Zuppiroli, L.; Graetzel, M. *J. Am. Chem. Soc.* **2003**, *125*, 8790−8797.
(6) (a) Sutin, N. *Acc. Chem. Res.* **1968**, *1*, 225. (b) Meyer, T. J. *Acc. Chem. Res.* **1978**, *11*, 94. (c) Schmid, B.; Garces, F. O.; Watts, R. J. *Inorg. Chem.* **1994**, *32*, 9.
(7) (a) Belmore, K. A.; Vanderpool, R. A.; Tsai, J.-C.; Khan, M. A.; Nicholas, K. M. *J. Am. Chem. Soc.* **1988**, *110*, 2004. (b) Silaware, N. D.; Goldman, A. S.; Ritter, R.; Tyler, D. R. *Inorg. Chem.* **1989**, *28*, 1231, 1488.
(8) (a) Demas, J. N.; Harris, E. W.; McBride, R. P. *J. Am. Chem. Soc.* **1977**, *99*, 3547. (b) Demas, J. N.; Harris, E. W.; Flynn, C. M.; Diemente, D. *J. Am. Chem. Soc.* **1975**, *97*, 3838. (c) Gao, R.; Ho, D. G.; Hernandez, B.; Selke, M.; Murphy, D.; Djurovich, P. I.; Thompson, M. E. *J. Am. Chem. Soc.* **2002**, *124*, 14828.
(9) Lo, K. K. W.; Ng, D. C. M.; Chung, C. K. *Organometallics* **2001**, *20*, 4999−5001.
(10) Polson, M.; Fracasso, S.; Bertolasi, V.; Ravaglia, M.; Scandola, F. *Inorg. Chem.* **2004**, *43*, 1950−1956.

10.1021/ic049277g CCC: $30.25
Published on Web 02/05/2005

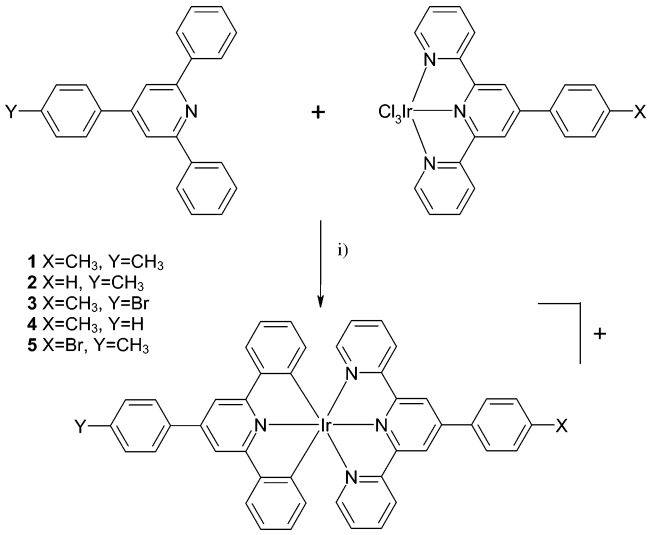

Figure 1. Reaction for the synthesis of axially substituted complexes. Key: (i) ethylene glycol, Ar, $AgNO_3$, 200 °C.

2:2′,6′:2″-terpyridine) and a C∧N∧C-bonded dppy derivative (dppy = 2,6-diphenylpyridine). This axially symmetric, heteroleptic arrangement gives the low-lying excited states of the molecule a unique directional nature. This article expands the previous work, with the synthesis and characterization of a series of axially substituted complexes with the same coordination arrangement being described (Figure 1). In principle, the study of spectroscopic and photophysical properties as a function of ligand substituents can give insight into nature of the excited states.[11,12] The main purpose of this work, however, is to present an extensive investigation of the excited states of these cyclometalated complexes by computational (DFT and TDDFT) techniques.

Computational techniques are gaining in importance in the elucidation and prediction of the photophysical properties of metal complexes. In the past, studies were limited due to the large size (in terms of electrons) of the complexes of interest, along with the difficulties involved in the accurate calculation of electron correlation effects. HF methods cannot account for the electron correlation contribution, while post-HF methods, for example the configuration interaction with single excitations (CIS) approach,[13] tend to scale poorly with an increasing number of electron (with calculation time increasing with N^6 or worse) making them too expensive in terms of computational cost to apply to metal complexes. In general, previous theoretical work applied mainly semiempirical methods (ZINDO, PM3).[14] Then again, DFT[15] has become a useful tool in evaluating ground-state properties with an accuracy close to that of post-HF methods. As a result, there is increasing interest in extending DFT to excited electronic states. Some studies have been conducted using DFT which have involved various cyclometalated Ir complexes.[16] Essentially they clarified the distinct nature of the transitions that yield the peculiar characteristics of these compounds. Nevertheless, very little theoretical work is yet available on this topic despite the potential interest of an advanced quantum chemical approach for a better understanding of key issues, like the nature of both the ground and the excited states involved in the absorption and/or emission. Tests on the time-dependent DFT (TDDFT) approach, also including hybrid HF/DFT methods, have already proved to supply results for low excitation energies usually superior to those obtained by time-dependent HF or by the CIS methods.

Experimental Section

Preparation of Compounds. [(4′-Phenyl-2:2′,6′:2″-terpyridine)-$IrCl_3$], [(4′-(4-bromophenyl)-2:2′,6′:2″-terpyridine)$IrCl_3$], and [(4′-(4-tolyl)-2:2′,6′:2″-terpyridine)$IrCl_3$] were synthesized according to the method of Collin et al.[17] in 65, 72, and 76% yield, respectively. 2,6-Diphenyl-4-(4-tolyl)pyridine, 2,4,6-triphenylpyridine, and 2,6-diphenyl-4-(4-bromophenyl)pyridine were synthesized in a single step by the method of Cave et al.[18] in 56, 76, and 67% yield, respectively. [(4′-(4-Bromophenyl)-2:2′,6′:2″-terpyridine)Ir(2,6-diphenyl-4-(4-tolyl)pyridine)](NO_3), **5**, was synthesized as previously reported.[10] Physical properties agreed with the literature values.

General Procedure for Complex Synthesis. A suspension of the appropriate Ir precursor (0.14 mmol), the cyclometalating ligand (0.15 mmol), and $AgNO_3$ (130 mg, excess) was heated to 190 °C in degassed ethylene glycol in the absence of direct light. On cooling, the suspension was filtered through Celite to remove AgCl and a black byproduct. The Celite plug was washed extensively with methanol. The organic solutions were combined and evaporated to remove the methanol. Water was added to precipitate the crude product, which was collected by filtration. The pure product was isolated by column chromatography on SiO_2 (prepared with an acetonitrile/saturated aqueous KNO_3 (10:1) solution), eluting with neat acetonitrile. The first eluted orange band was extracted with water and dichloromethane. The aqueous layer was discarded, and the organic layer was rotovaped to dryness. The residue was dissolved in a minimum of acetonitrile, the solution was filtered, and a solid was precipitated by addition to water. The pure product was collected by filtration and air-dried. NMR and mass spectral data are given below for each complex. Full NMR spectra and electrospray mass spectra are reported as Supporting Information.

[(4′-(4-Tolyl)-2:2′,6′:2″-terpyridine)Ir(2,6-diphenyl-4-(4-tolyl)-pyridine)](NO_3) (1). Yield: 31 mg (23%). ^{1}H NMR (400 MHz,

(11) (a) Page, S. E.; Flood, A.; Gordon, K. C. *J. Chem. Soc., Dalton Trans.* **2002**, *6*, 1180−1187. (b) Waterland, M. R.; Flood, A.; Gordon, K. C. *J. Chem. Soc., Dalton Trans.* **2000**, *2*, 121−127.

(12) *Inorganic and Electronic Spectroscopy, Volume II, Applications and Case Studies*; Soloman, E. I., Lever, A. B. P., Eds.; J. Wiley and Sons Inc.: New York, 1999.

(13) (a) Tozer, D. J.; Handy, N. C. *J. Chem. Phys*. **1998**, *109*, 10180. (b) Matsuzawa, N. N.; Ishitani, A.; Dixon, D. A.; Uda, T. *J. Phys. Chem. A* **2001**, *105*, 4953. (c) Boulet, P.; Chermette, H.; Daul, C.; Gilardoni, F.; Rogemond, F.; Weber, J.; Zuber, G. *J. Phys. Chem. A* **2001**, *105*, 885. (d) Cavillot, V.; Champagne, B. *Chem. Phys. Lett.* **2002**, *354*, 449.

(14) (a) Wolfbauer, G..; Bond, AM..; Deacon, G. B.; MacFarlane, D. R.; Spiccia, L. *J. Am. Chem. Soc*. **2000**, *122*, 130−142. (b) Rensmo, H.; Lunell, S.; Siegbahn, H. J. *Photochem. Photobiol. A* **1998**, *114*, 117. (c) Nazeeruddin, Md. K.; Zakeeruddin, S. M.; Humphry-Baker, R.; Gorelsky, S. I.; Lever, A. B. P.; Gratzel, M. *Coord. Chem. Rev*. **2000**, *208*, 213.

(15) Koch, W.; Holthausen, M. C. *A Chemist's Guide to Density Functional Theory*; Wiley-VCH: Weinheim, Germany, 2000.

(16) Lamansky, S.; Djurovich, P.; Murphy, D.; Abdel-Razzaq, F.; Kwong, R.; Tsyba, I.; Bortz, M.; Mui, B.; Bau, R.; Thompson, M. E. *Inorg. Chem*. **2001**, *40*, 1704.

(17) Collin, J.-P.; Dixon, I. M.; Sauvage, J.-P.; Williams, J. A. G.; Barigelletti, F.; Flamigni, L. *J. Am. Chem. Soc*. **1999**, *121*, 5009−5016.

(18) Cave, G. W. V.; Raston, C. L. *J. Chem. Soc., Perkin Trans. 1* **2001**, 3258.

CD_3CN): δ 8.95 (s, $H_{T3',5'}$, 2H), 8.64 (d, $J^d = 8.0$ Hz, H_{T3}, 2H), 8.30 (s, $H_{D3',5'}$, 2H), 8.08 (d, $J^d = 8.0$ Hz, H_{Tc}, 2H), 8.03 (d, $J^d = 7.0$ Hz, H_{Dc}, 2H), 8.01 (d, $J^d = 7.5$ Hz, H_{D3}, 2H), 7.98 (td, $J^t = 6.5$ Hz, $J^d = 1.0$ Hz, H_{T4}, 2H), 7.87 (d, $J^d = 5.0$ Hz, H_{T6}, 2H), 7.57 (d, $J^d = 7.0$ Hz, H_{Tb}, 2H), 7.54 (d, $J^d = 7.5$ Hz, H_{Db}, 2H), 7.27 (ddd, $J^d = 7.0$ Hz, $J^d = 6.0$ Hz, $J^d = 1.0$ Hz, H_{T5}, 2H), 7.01 (td, $J^t = 7.0$ Hz, $J^d = 0.5$ Hz, H_{D4}, 2H), 6.78 (td, $J^t = 7.0$ Hz, $J^d = 1.0$ Hz, H_{D5}, 2H), 6.29 (d, $J^d = 8.0$ Hz, H_{D6}, 2H), 2.53 (s, H_{Ta}, H_{Da}, 6H). ^{13}C NMR (100 MHz, CD_3CN): δ 166.8, 165.0, 158.2, 153.5, 152.9, 151.1, 148.0, 147.8, 141.8, 141.7, 138.4, 135.5, 134.9, 134.6, 131.2, 130.9(2C), 128.7(2C), 128.3, 126.9, 125.9, 124.9, 122.5, 115.1, 21.3 (2C). MS (ESI): m/z 836.0 ($[M - NO_3]^+$ requires m/z 836.0).

[(4′-(Phenyl)-2:2′,6′:2″-terpyridine)Ir(2,6-diphenyl-4-(4-tolyl)-pyridine)](NO$_3$) (2). Yield: 27 mg (20%). ^{1}H NMR (400 MHz, CD_3CN): δ 8.98 (s, $H_{T3',5'}$, 2H), 8.66 (d, $J^d = 6.0$ Hz, H_{T3}, 2H), 8.30 (s, $H_{T3',5'}$, 2H), 8.20 (d, $J^d = 8.0$ Hz, H_{Tc}, 2H), 8.03 (d, $J^d = 7.0$ Hz, H_{Dc}, 2H), 8.01 (d, $J^d = 8.0$ Hz, H_{D3}, 2H), 7.98 (t, $J^t = 6.5$ Hz, H_{T4}, 2H), 7.87 (d, $J^d = 8.0$ Hz, H_{T6}, 2H), 7.76 (dd, $J^d = 7.0$ Hz, $J^d = 1.0$ Hz, H_{Tb}, 2H), 7.68 (d, $J^d = 7.5$ Hz, H_{Db}, 1H), 7.54 (d, $J^d = 7.0$ Hz, H_{Db}, 2H), 7.27 (ddd, $J^d = 7.0$ Hz, $J^d = 6.0$ Hz, $J^d = 1.0$ Hz, H_{T5}, 2H), 7.01 (ddd, $J^d = 7.0$ Hz, $J^d = 7.0$ Hz, $J^d = 0.5$ Hz, H_{D4}, 2H), 6.78 (ddd, $J^d = 7.0$ Hz, $J^d = 6.5$ Hz, $J^d = 1.0$ Hz, H_{D5}, 2H), 6.30 (ddd, $J^d = 6.0$ Hz, $J^d = 6.0$ Hz, $J^d = 0.5$ Hz, H_{D6}, 2H), 2.54 (s, H_{Da}, 3H). ^{13}C NMR (100 MHz, CD_3CN): δ 166.8, 165.0, 158.2, 153.6, 152.9, 151.0, 148.0, 147.9, 141.7, 138.4, 137.9, 135.5, 134.6, 131.2, 130.9, 130.8, 130.6, 128.8, 128.7, 128.3, 126.9, 126.0, 125.0, 122.9, 115.1, 20.5. MS (ESI): m/z 821.2 ($[M - NO_3]^+$ requires m/z 821.7).

[(4′-(4-Tolyl)-2:2′,6′:2″-terpyridine)Ir(2,6-diphenyl-4-(4-bromophenyl)pyridine)](NO$_3$) (3). Yield: 24 mg (15%). ^{1}H NMR (400 MHz, CD_3CN): δ 8.95 (s, $H_{T3',5'}$, 2H), 8.64 (d, $J^d = 8.0$ Hz, H_{T3}, 2H), 8.29 (s, $H_{D3',5'}$, 2H), 8.08 (d, $J^d = 7.5$ Hz, H_{Tc}, 2H), 8.04 (d, $J^d = 7.5$ Hz, H_{Dc}, 2H), 8.01 (d, $J^d = 8.0$ Hz, H_{D3}, 2H), 7.98 (td, $J^t = 6.5$ Hz, $J^d = 1.5$ Hz, H_{T4}, 2H), 7.89 (d, $J^d = 8.0$ Hz, H_{Db}, 2H), 7.85 (dd, $J^d = 7.0$ Hz, $J^d = 1.0$ Hz, H_{T6}, 2H), 7.58 (d, $J^d = 7.5$ Hz, H_{Tb}, 2H), 7.27 (ddd, $J^d = 7.0$ Hz, $J^d = 6.0$ Hz, $J^d = 1.0$ Hz, H_{T5}, 2H), 7.01 (td, $J^t = 7.0$ Hz, $J^d = 0.5$ Hz, H_{D4}, 2H), 6.79 (td, $J^d = 7.5$ Hz, $J^d = 1.0$ Hz, H_{D5}, 2H), 6.30 (dd, $J^d = 6.0$ Hz, $J^d = 0.5$ Hz, H_{D6}, 2H), 2.54 (s, H_{Ta}, 3H). ^{13}C NMR (100 MHz, CD_3CN): δ 166.3, 164.4, 157.5, 152.2, 151.6, 150.3, 147.1, 147.0, 141.1, 137.8, 137.7, 136.9, 134.2, 133.9, 132.6, 130.5, 130.3, 130.0, 127.9, 127.5, 126.2, 125.2, 124.2, 121.8, 114.5, 20.6. MS (ESI): m/z 899.6 ($[M - NO_3]^+$ requires m/z 899.1).

[(4′-(4-Tolyl)-2:2′,6′:2″-terpyridine)Ir(2,4,6-triphenylpyridine)](NO$_3$) (4). Yield: 45 mg (35%). ^{1}H NMR (400 MHz, CD_3CN): δ 8.94 (s, $H_{T3',5'}$, 2H), 8.64 (dd, $J^d = 7.0$ Hz, $J^d = 0.5$ Hz, H_{T3}, 2H), 8.31 (s, $H_{D3',5'}$, 2H), 8.13 (d, $J^d = 7.5$ Hz, H_{Dc}, 2H), 8.09 (d, $J^d = 7.0$ Hz, H_{Tc}, 2H), 8.02 (d, $J^d = 7.0$ Hz, H_{D3}, 2H), 7.98 (td, $J^t = 7.0$ Hz, $J^d = 1.0$ Hz, H_{T4}, 2H), 7.86 (dd, $J^d = 5.5$ Hz, $J^d = 0.5$ Hz, H_{T6}, 2H), 7.73 (t, $J^t = 7.0$ Hz, H_{Db}, 2H), 7.64 (t, $J^t = 7.0$ Hz, H_{Da}, 1H), 7.58 (d, $J^d = 7.5$ Hz, H_{Tb}, 2H), 7.27 (ddd, $J^d = 7.0$ Hz, $J^d = 6.0$ Hz, $J^d = 1.0$ Hz, H_{T5}, 2H), 7.01 (td, $J^t = 7.0$ Hz, $J^d = 0.5$ Hz, H_{D4}, 2H), 6.78 (td, $J^t = 7.0$ Hz, $J^d = 1.0$ Hz, H_{D5}, 2H), 6.30 (d, $J^d = 6.0$ Hz, H_{D6}, 2H), 2.54 (s, H_{Ta}, 3H). ^{13}C NMR (100 MHz, CD_3CN): δ 166.2, 164.3, 157.5, 152.9, 152.2, 150.3, 147.2, 147.1, 141.1, 140.5, 137.7, 135.2, 134.3, 133.9, 130.5, 130.2, 129.6, 128.1, 128.0, 127.5, 126.2, 125.2, 124.2, 121.8, 114.7, 20.6. MS (ESI): m/z 821.2 ($[M - NO_3]^+$ requires m/z 821.7).

Apparatus and Procedures. General procedures have been reported previously.[10] Apparatus for femtosecond spectroscopy has also been described previously.[19] Areas (and hence relative oscillator strengths) were measured by fitting pure Gaussian curves directly to the electronic absorption spectra in wavenumbers.

Computational Details. Calculations on the electronic ground state of the complex were carried out using B3LYP functional within the density functional theory method.[20] "Double-ζ" quality basis sets were employed for the ligands (6-31G) and Ir (LANL2DZ). A relativistic effective core potential (ECP) on Ir[21] replaced the inner core electrons leaving the outer core [$(5s)^2(5p)^6$] electrons and the $(5d)^6$ valence electrons of Ir(III). The geometries were fully optimized without symmetry constraints. At the respective ground-state geometries, time-dependent DFT (TDDFT) calculations were performed at the same level of accuracy as specified above. Triplet-state unrestricted optimization was carried out using the same approach applied for the ground state.[21,22] Again, no geometry constraints were imposed. All calculations were preformed using Gaussian 98 software package.[23] The program MOLDEN 3.9 was used to visualize the orbitals.[24] 3D representation of the spin density was plotted with MOLEKEL 4.3.[25]

Results and Discussion

Synthesis. The synthesis of these new complexes was achieved in ethylene glycol at 200 °C for 1 h (Figure 1). The reaction required vigorous degassing with argon and silver to remove the chloride ions. Exposure to low levels of light did not seem to affect the yield of the reaction. These reaction conditions are harsh, even for iridium complexes, which are notorious for requiring high temperatures to overcome the inertness of the coordination sphere. In the case of iridium bis(terpyridine) complexes, temperatures are required to be high (140−180 °C) and yet strictly controlled to stop the formation of cyclometalated complexes. Light must also be strictly excluded for the same reason. Here, no reaction can be seen at less than 180 °C and the product is formed under the same conditions found to favor cyclometalated products in bis(terpyridine) reactions. The yields of the reactions range from low to moderate. There seems to be no discernible reason for the variation in the yields on the basis of the nature of the diphenyl or terpyridine ligand. However significant variation was seen between different

(19) Chiorboli, C.; Rodgers, M. A. J.; Scandola, F. *J. Am. Chem. Soc.* **2003**, *125* (2), 483−491.

(20) (a) Lee, C.; Yang, W.; Parr, R. G. *Phys. Rev. B* **1988**, *37*, 785. (b) Becke, A. D. *J. Chem. Phys.* **1993**, *98*, 5648. (c) Jeffrey Hay, P. *J. Phys. Chem. A* **2002**, *106*, 1634−1641.

(21) Hay, P. J.; Wadt, W. R. *J. Chem. Phys.* **1985**, *82*, 299−310.

(22) Guillemoles, J. F.; Barone, V.; Joubert, L.; Adamo, C. *J. Phys. Chem. A* **2002**, *106* (46), 11354−11360.

(23) Frisch, M. J.; Trucks, G. W.; Schlegel, H. B.; Scuseria, G. E.; Robb, M. A.; Cheeseman, J. R.; Zakrzewski, V. G.; Montgomery, J. A.; Stratmann, R. E.; Burant, J. C.; Dapprich, S.; Millam, J. M.; Daniels, A. D.; Kudin, K. N.; Strain, M. C.; Farkas, O.; Tomasi, J.; Barone, V.; Cossi, M.; Cammi, R.; Mennucci, B.; Pomelli, C.; Adamo, C.; Clifford, S.; Ochterski, J.; Petersson, G. A.; Ayala, P. Y.; Cui, Q.; Morokuma, K.; Malick, D. K.; Rabuck, A. D.; Raghavachari, K.; Foresman, J. B.; Cioslowski, J.; Ortiz, J. V.; Stefanov, B. B.; Liu, G.; Liashenko, A.; Piskorz, P.; Komaromi, I.; Gomperts, R.; Martin, R. L.; Fox, D. J.; Keith, T.; Al-Laham, M. A.; Peng, C. Y.; Nanayakkara, A.; Gonzalez, C.; Challacombe, M.; Gill, P. M. W.; Johnson, B. G.; Chen, W.; Wong, M. W.; Andres, J. L.; Head-Gordon, M.; Replogle, E. S.; Pople, J. A. *Gaussian 98*, revision A.11; Gaussian, Inc.: Pittsburgh, PA, 1998.

(24) Schaftenaar, G.; Noordik, J. H. Molden: a pre- and post-processing program for molecular and electronic structures. *J. Comput.-Aided Mol. Des.* **2000**, *14*, 123−134.

(25) Flükiger, H. P.; Lüthi, S.; Portmann, J.; Weber, P. *MOLEKEL 4.3*; Swiss Center for Scientific Computing: Manno, Switzerland, 2000−2002. Portmann, S.; Lüthi, H. P. MOLEKEL: An Interactive Molecular Graphics Tool. *CHIMIA* **2000**, *54*, 766−770.

Table 1. Electrochemistry and Electronic Absorption[a]

compd	redn/V[b]	oxidn/V[b]	electronic abs spectra: λ/nm ($\epsilon/10^{-3}$ mol^{-1} cm^{-1})
1	−1.29 (95), −1.76 (irrev)	1.08 (95), 1.45 (irrev)	282 (93.1), 323[c] (59.2), 437 (15.0), 481[c] (10.9), 515 (9.2)
2	−1.27 (105), −1.85 (irrev)	1.09 (110), 1.45 (irrev)	283 (84.7), 322[c] (51.1), 436 (15.4), 480[c] (11.7), 517 (9.7)
3	−1.29 (60), −1.67 (irrev)	1.07 (65), 1.35 (irrev)	283 (96.4), 324[c] (55.1), 436 (14.9), 483[c] (10.8), 515 (9.0)
4	−1.29 (60), −1.70 (irrev),	1.06 (60), 1.39 (irrev)	281 (81.4), 321[c] (53.4), 434 (14.2), 480[c] (10.1), 514 (8.7)
5	−1.24 (95), −1.83 (irrev)	1.08 (90), 1.41 (irrev)	283 (86.3), 323[c] (53.7), 437 (15.0), 482[c] (10.9), 514 (9.2)
$[Ir(ppy)_2(bpy)]^+$ [d]	−1.37, −2.02	1.26	265 (32), 310 (16), 375 (4.7), 410 (2.8), 465 (0.58)
$[Ir(ttp)_2]^{3+}$ [e]	−0.81, −0.91[f]	*g*	205 (77.4), 251 (62.3), 278 (45.9), 305 (46.2), 371 (43), 347 (36.8), 373 (29.0)

[a] Recorded in degassed acetonitrile. [b] Vs SCE; $E_{1/2}$ values; anodic/cathodic peak separations in parentheses for reversible processes; peak potentials for irreversible (irrev) processes. [c] Shoulder. [d] Reference 27. [e] Reference 17. [f] In DMF. [g] Unseen within solvent window.

reactions to synthesize the same complex but using different batches of the terpyIrCl$_3$ compound. As this complex is largely uncharacterized, we suspect variation in the quality of this species to be the cause of both the poor and variable yields. This species has been replaced in the past with a bis-(*tert*-butyl) derivative to increase solubility and hence allow for purification.[17] Due to future requirements for these molecules (i.e. an unencumbered 4 position on the pendant phenyl ring) this option is not open to us.

Electrochemistry. The complexes exhibit two reversible electrochemical processes. The data from the cyclic voltammetry are collected in Table 1. At negative potentials there is a single one-electron process at approximately −1.30 V. We assign this process to the reduction of the terpyridine ligand. This assignment is supported by DFT calculations that show that the LUMO is mainly localized on the terpyridine ligand (vide infra). The observation of the reduction occurring predominantly on the nitrogen-rich ligand of a cyclometalated complex has also been found for some rhodium complexes and has also been supported by DFT calculations.[26] The reduction potential changes only slightly with substitution on the terpyridine ligand and not at all with variation of the cyclometalating ligand. The changes follow the expected trend with the electron-donating group (CH_3, complexes **1**, **3**, and **4**) have the most negative reduction potential (−1.29 V), then the intermediate group (H, complex **2**, −1.27 V), and finally the electron-withdrawing group (Br, complex **5**, −1.24 V). This tends to confirm the reduction is occurring on the terpyridine ligand. At more negative potentials, approximately −1.75 V, the complexes undergo an irreversible process. This is similar to the potentials at which the complexes Pt(dppy)Cl and Pd(dppy)Cl undergo their first reduction[27] and have hence been assigned as the reduction of the diphenylpyridine ligand.

There is also a reversible one-electron oxidation at +1.08 V. The potential does not change either with variation of the cyclometalating ligand or with variation of the terpyridine ligand. This potential cannot be simply assigned to metal oxidation, due to the strong covalency of the Ir−C bonds. In fact, DFT calculations show that the highest occupied molecular orbitals of **2** and **4** are substantially delocalized over the Ir−dppy fragment (vide infra). Arguments can be made about the potential of this process similar to those that have been made previously for complex **5** when compared to similar compounds such as $[Ir(ttp)_2]^{3+}$ and $[Ir(ppy)_2(bpy)]^+$.[10,17,28] A second, irreversible process at more positive potentials remains unassigned but is more likely a second process occurring on the dppy−metal moiety than an oxidation of the terpyridine unit, which is not seen in other complexes within the solvent window (<+2.3 V for acetonitrile).

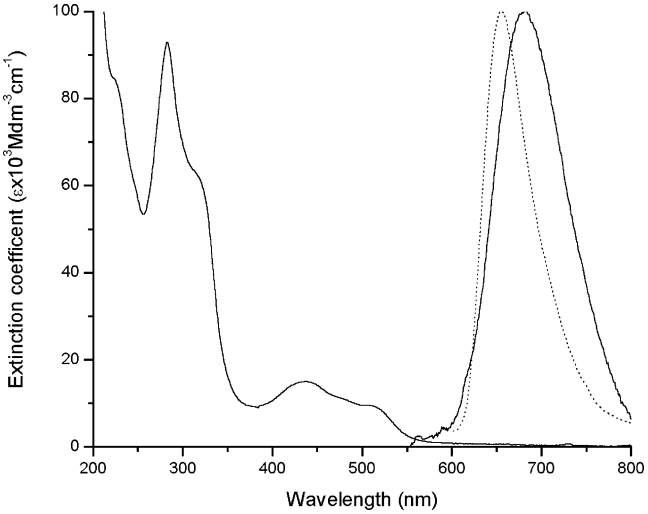

Figure 2. Absorption (left) and emission spectra (right, normalized, arbitrary units) (293 K, continuous line; 77 K, dotted line) of complex **1**.

Electronic Absorption Spectrum. The electronic absorption spectrum of **1** is shown in Figure 2.

Spectroscopic data for all the complexes are summarized in Table 1. There are two strong absorptions in the UV region (ca. 280 and 320 nm) that can be assigned as ligand-centered (LC) $\pi-\pi^*$ transitions. Less usually for iridium cyclometalated complexes, a well-resolved band system is observed in the visible region with two maxima and a shoulder (ca. 435, 515, and 480 nm). Comparisons between these compounds and similar cyclometalated complexes are as for the previously reported complex.[10] These absorptions show almost no variation in energy with substitution, and differences in their intensities are within experimental error. The detailed assignment of these absorptions will be discussed in light of DFT calculations (vide infra).

Emission Measurements. The emission spectra of **1** at 298 and 77 K are shown in Figure 2. Emission data for complexes **1**−**5** are reported in Table 2. As previously

(26) Ghizdavu, L.; Lentzen, O.; Schumm, S.; Brodkorb, A.; Moucheron, C.; Kirsch-De Mesmaeker, A. *Inorg. Chem.* **2003**, *42*, 1935−1944.
(27) Yam, V. W. W.; Tang, R. P. L.; Wong, K. M. C.; Lu, X. X.; Cheung, K. K.; Zhu, N. *Chem.*−*Eur. J.* **2002**, *8*, 4066.
(28) Ohsawa, Y.; Sprouse, S.; King, K. A.; DeArmond, M. K.; Hanck, K. W.; Watts, R. J. *J. Phys. Chem.* **1987**, *91*, 1047.

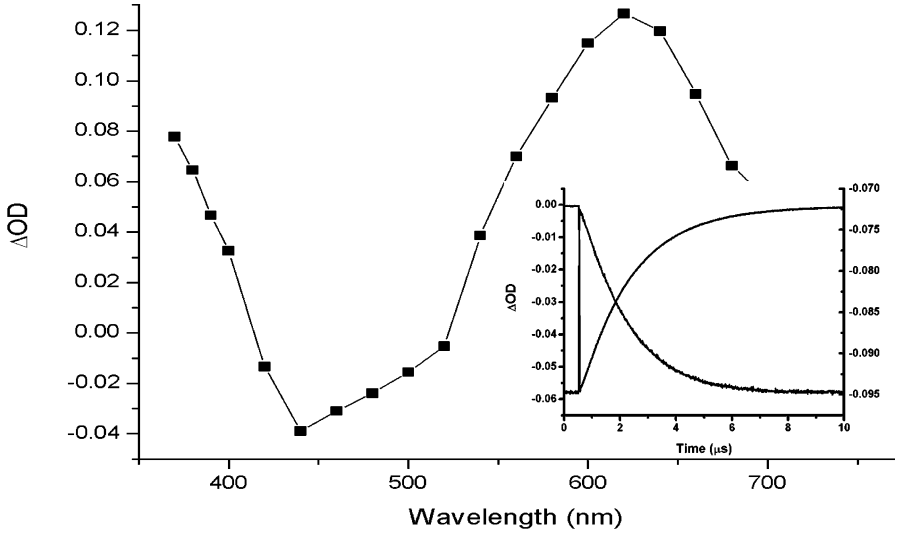

Figure 3. Transient differential absorption spectrum of complex **1** recorded in degassed acetonitrile solution approximately 50 ns after the laser pulse (λ_{ex} = 355 nm). Inset: Decay of the transient at 620 nm (dropping trace, left scale) as compared with the emission decay (λ_{em} = 680 nm, rising trace, right scale).

Table 2. Emission Properties Measured in Aerated Acetonitrile

compd	λ_{em}/nm (77 K)[a]	λ_{em}/nm (RT)[b]	τ/ns (RT)	τ/μs (RT)[c]	ϕ (RT)[c]
1	655	680	195	1.83	0.033
2	657	684	192	1.63	0.027
3	654	680	212	1.76	0.032
4	654	679	196	2.05	0.028
5	662	689	198	1.68	0.035
$[Ir(ppy)_2(bpy)]^+$ [d]	510	606		0.337	
$[Ir(ttp)_2]^{3+}$ [e]	494	506	2400	9.5	0.029

[a] 4:1 methanol/ethanol. [b] RT = room temperature. [c] Deaerated with argon. [d] Reference 27. [e] Reference 17.

proposed for **5**,[10] and as discussed in detail later on (vide infra), the emitting excited state of complexes **1**−**5** has a partial dppy → tpy LLCT character. Accordingly, the energy of the emission is dependent on the nature of the substituent on the tpy-type ligand, with a definite (though small) red shift in going from electron donating to electron donating−withdrawing, e.g. **1** > **2** > **5** in Table 2. This is due to the stabilization/destabilization of the terpyridine π^* acceptor orbital by electron-withdrawing/-donating groups. The small magnitude of the effect is consistent with the very small amplitude of this orbital at the position of the substituents (vide infra). Effects of substitution at the dppy-like ligand, if any, are much less evident (e.g., **1** = **3** ≈ **4** in Table 2). At low temperature (77 K) the emissions remain broad and have the same variation of energy with substituents as at room temperature. The shifts in emission energy, on moving to lower temperature, are approximately 610 cm^{-1} and are similar to that of $Ru(ttp)_2^{2+}$ (600 cm^{-1})[29] implying that it has a similar CT excited state. They are however lower than those of other Ir complexes believed to have CT excited state (e.g. $[Ir(bipy)(ppy)_2]^+$ has a blue shift of 2300 cm^{-1}).[30]

The emission quantum yields of the complexes (Table 2) are all around 0.03, i.e., uniformly low (by ca. 1 order of magnitude) with respect to several previously reported cyclometalated complexes.[4] As the lifetimes (ca. 2 μs) are similar to that of the highly emissive complex$(ppy)_2Ir(acac)$,[4] these complexes must have low radiative decay rates (ca. 10^{-4} as compared to 10^{-5} s^{-1}). Possible reasons for this will be discussed in the light of the computational results (vide infra).

Transient Absorption Measurements. The transient electronic absorption spectrum of the complexes, collected in degassed acetonitrile solution at room temperature, are shown in Figure 3. The data points were measured approximately 50 ns after the laser pulse. The decay matches well with the emission decay, indicating that the transient spectrum is associated with the emissive state. Three features are clearly visible. First, there is a strong absorption in the UV region with a maximum at less than 360 nm. There is also a strong absorption in the red region with a maximum at approximately 610 nm. Finally, there is bleaching in the visible region of a series of bands at 440, 488, and 521 nm. The bleaching features correspond very closely to the ground-state absorptions in the visible region (see Figure 2). The two absorption features are characteristic of the formation of the radical anion of a phenyl-substituted terpyridine ligand,[31] providing direct spectroscopic evidence for the terpyridine-localized nature of the LUMO.

In picosecond experiments on **1**, also conducted in acetonitrile, a constant spectrum identical with that observed

(29) Hammarstrom, L.; Barigelletti, F.; Flamigni, L.; Indelli, M. T.; Armaroli, N.; Calogero, G.; Guardigli, M.; Sour, A.; Collin, J.-P.; Sauvage, J.-P. *J. Phys. Chem. A.* **1997**, *101* (48), 9061−9069.
(30) Garces, F. O.; King, K. A.; Watts, R. J. *Inorg. Chem.* **1988**, *27*, 3464.
(31) Collin, J.-P.; Guillerez, S.; Sauvage, J.-P.; Barigelletti, F.; De Cola, L.; Flamigni, L.; Balzani, V. *Inorg. Chem.* **1991**, *30*, 4230.

Table 3. Comparison of Calculated Bond Lengths and Valence Angles for Compound **2** with Experimental Values from X-ray Diffraction on the Analogous Compound **5**[10]

dist	crystallogr data/Å	calcd data/Å	angle	crystallogr data/deg	calcd data/deg
Ir−N1	1.943(6)	1.96	N1−Ir−N4	177.6(2)	180
Ir−N2	2.044(6)	2.06	N2−Ir−N3	159.9(3)	160
Ir−N3	2.053(6)	2.06	C5−Ir−C6	158.3(3)	158
Ir−N4	2.022(6)	2.05	N1−Ir−C6	103.4(3)	101
Ir−C5	2.122(8)	2.11	N2−Ir−C5	93.5(3)	92
Ir−C6	2.094(8)	2.11	N3−Ir−N4	98.7(2)	100

Table 4. Computed TDDFT Vertical Excitations Energies (nm) and Relative Oscillator Strength (*f*) for the Lowest Singlet Excited States of Compounds **4** and **2**[a]

compd	principal transitn[b]	assgnt	calcd energy/nm (*f*)[c]	exptl energy[d]/nm (*f*)[c]
4	$S_0 \rightarrow S_1$	HOMO → LUMO	550 (0)	
	$S_0 \rightarrow S_2$	HOMO → LUMO+1	521 (10)	515 (20)
	$S_0 \rightarrow S_3$	HOMO-1 → LUMO+1	518 (4)	481 (2)
	$S_0 \rightarrow S_4$	HOMO-1 → LUMO	472 (46)	436 (76)
2	$S_0 \rightarrow S_1$	HOMO → LUMO	555 (0)	
	$S_0 \rightarrow S_2$	HOMO-1 → LUMO+1	520 (10)	514 (25)
	$S_0 \rightarrow S_3$	HOMO → LUMO+1	522 (4)	481 (2)
	$S_0 \rightarrow S_4$	HOMO-1 → LUMO	471 (44)	434 (95)

[a] Orbital labeling is referred to Figure 4. [b] Excited states are described by combinations of one-electron excitations (see text and footnote 33). [c] Relative oscillator strength. [d] Relative band area.

in the nanosecond time regime is already reached after 2 ps. A minor ultrafast process (time constant ca. 200 fs, ca. 10% increase in 610-nm optical density) is probably associated with vibrational relaxation in the lowest excited state. Planarization of the tolyl fragment upon relaxation in the excited state (a possibility that could be envisaged on the basis of similar effects reported for ruthenium phenylbipyridine complexes[32]) is not supported by the results of DFT calculations (vide infra).

Computational Results. The calculated structures correspond excellently with the crystallographic data and, along with the orbital description, accurately depict the ground-state structure of these complexes. Some comparisons between the ground-state-optimized geometry of **2** and the crystal structure of **5** are given in Table 3. The geometries of **2** and **4** are almost identical, with all distances and angles agreeing within experimental error. In both cases the pendant phenyl ring is twisted out of the plane of the terpyridine ligand by 35 and 37° in **2** and **4**, respectively.

TDDFT calculations are particularly well suited to low-energy valence excited states which can be described by combinations of single excitations.[33] In particular, TDDFT results for excitations with an energy less than half of the ionization potential are almost comparable in accuracy to the sophisticated CAS-PT2 calculations,[34] with energy differences between experimental and calculated values within 0.4 eV. The three transitions observed in the visible regions of the electronic absorption spectra compare well with three calculated transitions (Table 4). These transitions, leading to S_2, S_3, and S_4 excited states, essentially consist of the combinations of transitions from the HOMO-1 and HOMO orbitals to the LUMO and LUMO+1 orbitals. The lowest energy transition ($S_0 \rightarrow S_1$, predominately HOMO → LUMO in character) was calculated to have a vanishingly small intensity and is not seen in the spectra. As shown in Figure 4, the HOMO and HOMO-1 are essentially localized on the Ir−dppy fragment and the LUMO and LUMO+1 on the Ir-tpy fragment. Therefore, while both the donor and acceptor orbitals have significant metal and ligand character, the main charge displacement takes place from the dppy-like to the tpy-like ligand. In simple terms, the spectroscopic states possess some dppy → tpy LLCT character. Similar results have recently been reported for a series of rhodium complexes, where the emitting state of the complexes of the type $[Rh(ppy)_2(TAP)]^+$ (TAP = 1,4,5,8-tetraazaphenanthrene) were also best described as LLCT in nature.[26] From this viewpoint, the low intensity of the $S_0 \rightarrow S_1$ transition can be likely associated to a symmetry restriction.[20] Charge-transfer

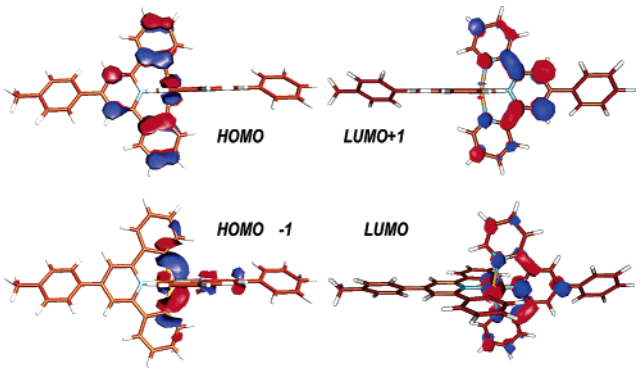

Figure 4. Isocontour plots of the two highest occupied and two lowest virtual MOs for compound **2** at ground-state equilibrium structure.

(32) Damrauer, N. H.; McCusker, J. K. *J. Phys. Chem. A.* **1999**, *103*, 8440−8446.

(33) TDDFT formalism regards excited states as linear combinations of singly excited determinants. Accordingly, each transition includes a series of excitations, where some of them outweigh the others and therefore characterize the transition. Nonetheless, identification of the transition with a single excitation might be misleading in some cases. As a matter of example, one may notice that in Table 4 the transition with the shortest wavelength ($S_0 \rightarrow S_4$) is described as a HOMO-1 → LUMO excitation, whereas transition $S_0 \rightarrow S_3$ is described as a HOMO-1 → LUMO+1 excitation. At first sight this is counterintuitive, but considering the small energy difference between the transitions (0.2 eV), the even smaller energy gap between the involved acceptor orbitals ($\Delta E_{LUMO+1-LUMO} = 0.02$ eV), and, finally, the nature of the transition (linear combination of single excitations), the results prove to be reasonable. See the Supporting Information for frontier orbital energies and details of one-electron transitions involved in low-energy excitations.

bands derive intensity mainly from transitions polarized in the direction of charge transfer.[35] If we consider the molecule as a whole as having a C_2 effective symmetry, the HOMO transforms as the irreducible representation *a*, while the LUMO transforms as *b*. Therefore, the symmetry species of the HOMO−LUMO transition ($a \rightarrow b$) is polarized perpendicularly to the direction of charge transfer (along the *z* axis) and thus is expected to have low oscillator strength.

Concerning the triplet state potential energy surface optimization, for computational time reasons we focused our attention on compound **2 (**compound **4** was likely to give very similar outcome). When the calculated structures of the ground state (S_0) and lowest excited state (T_1) are compared, relatively small geometry changes are observed (see Supporting Information for a complete listing of structural parameters).[36] The largest changes involve the Ir−N bonding. The three Ir−N bonds on the tpy ligand are lengthened by 0.01 Å and the Ir−N on the dppy ligand lengthens by 0.02 Å, while the Ir−C bonds remain the same. This forces the dppy ligand to "bow" around the long axis. The two ligands are also bent further away from 180° along the long axis. The lengthening of the Ir−N bonds can be understood considering that the acceptor orbital is essentially an antibonding combination of a d orbital of the metal (d_{xz}, taking the molecular axis as the *z* axis and the C−Ir−C bond as the *x* axis) and the LUMO orbital of the tpy ligand. Moreover, the two unpaired electrons exert repulsion on each other, pushing apart the actual locations where the electrons reside.[37] There are also changes in bond distances within the terpyridine ligand, consistent with the population of an orbital which has antibonding character within and bonding character between pyridine rings.[38] It is important to notice that there is no change in the twist angle of the phenyl ring on either ligand. This is in contrast to what is considered to occur in the MLCT excited states of phenyl-substituted polypyridine ruthenium complexes. For example, in $[Ru(dpbpy)_3]^{2+}$ (dpbpy = 4,4′-diphenyl-2,2′-bipyridine), excited-state ligand planarization has been deduced from ultrafast spectroscopy.[32]

To investigate the nature of the electronic transition involving ground and first excited triplet state, we performed a Mulliken population analysis of the spin and charge densities on the molecule. The spin density is obtained as the difference between α and β spin contributions to the total electron density. The charge-density difference is obtained as the difference in total electron density between the two states of interest. Figure 5 shows the two singly occupied molecular orbitals (SOMOs) of the T_1 state. In Figure 6 is shown the isocontour plot of the spin density associated to T_1 (green chicken wire), compared to the equiprobability surfaces of the lower and higher energy SOMOs (orange and emerald surfaces, respectively). Spin density is frequently approximated by the density of the singly occupied orbitals, but for the majority of cases this simple approach is not sufficient.[39]

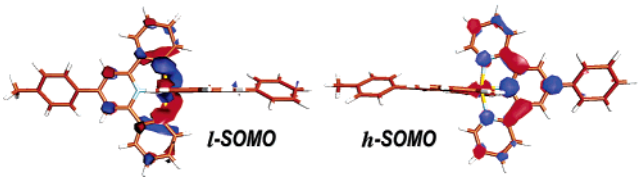

Figure 5. Isocontour plots of lowest (l) and highest (h) singly occupied molecular orbitals for compound **2**, at T_1 equilibrium geometry.

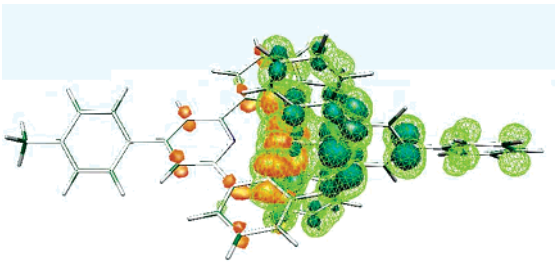

Figure 6. Contour plots of the spin density (green chicken wire), l-SOMO (orange), and h-SOMO (emerald) for T_1 equilibrium geometry of compound **2**.

The unpaired electrons, by virtue of the different interactions with electrons of different spin, spin-polarize the electron distribution in the closed shells. This process can add significant spin density at the position of the nuclei.[40] In our case spin density is reasonably, but not entirely, accounted for by the sum of the two SOMOs. Therefore, upon decay from T_1 to S_0, polarization of the spin will involve mainly recoupling of the electron in the higher SOMO (localized on the tpy ligand) with the electron residing in the lower SOMO (localized on the dppy ligand), as a genuine singlet state spin density is identically zero at every point in space. Spin and charge density are quite different in nature. Manifestation of the spin density in the three-dimensional Cartesian space can vary and redistribute over large distances with little energy. On the contrary, rearrangement of the classical charge density is energetically much more demanding. Figure 7 shows the electron density difference between excited and ground state. As the charge delocalization (and spin polarization) is rather structure insensitive, the T_1 equilibrium geometry was used when comparing T_1 and S_0 densities. Quite prominent charge

(34) Bauernschmitt, R.; Ahlrichs, R. *Chem. Phys. Lett.* **1996**, *256*, 454−464.
(35) Day, P.; Sanders, N. *J. Chem. Soc. A* **1967**, 1536.
(36) The potential energy surfaces (PES) of S_0 and T_1 are quite different. On S_0, minor geometrical rearrangements induce dramatic energy changes; on the contrary, remarkable geometrical modifications induce minor energy variations on T_1. Optimizations performed on flat PES are to be cautiously analyzed. The algorithm might actually wander on the surface for numerous optimization steps, making the location of the absolute minimum difficult. In the present case a modest geometrical rearrangement was obtained between S_0 and T_1 equilibrium geometries, indicating that a rather reliable optimization procedure was accomplished. With respect to the tolyl rotation, optimized geometry on T_1 with the related dihedral kept frozen showed an energy increase of 3 kcal mol^{-1} compared to the equilibrium geometry on the same PES. The result clarifies that the abovementioned is not a free rotation.
(37) Ai, H. Q.; Bu, Y. X.; Han, K. L. *J. Chem. Phys.* **2002**, *117*, 7593−7602.
(38) Hansen, P. W.; Jensen, P. W. *Spectrochim. Acta, Part A* **1994**, *50A*, 169−83.
(39) Novozhilova, I. V.; Volkov, A. V.; Coppens, P. *J. Am. Chem. Soc.* **2003**, *125*, 1079−1087.
(40) Munzarova, M. L.; Kubac×c1ek, P.; Kaupp, M. *J. Am. Chem. Soc.* **2000**, *122*, 11900−11913.

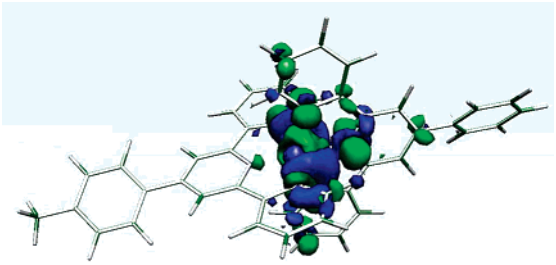

Figure 7. Contour plot of the difference in electron-density distribution between T_1 and S_0 states of compound **2**. Green (positive) areas show regions with higher electron density for the T_1 state, whereas blue (negative) areas indicate regions with higher electron density for S_0.

reorganization can be noted. Upon decay to the ground state, electron density is displaced from the plane defined by the tpy ligand to the perpendicular plane, defined by the dppy ligand (green areas indicate regions with higher electron density for T_1 state, whereas blue areas indicate regions with higher electron density for S_0). Quantitative examination of the change in the total charge distribution (including the nuclear charges) from the S_0 ground state to the T_1 excited state gives the following picture. The charge on the iridium center remains almost constant (e.g., +1.092 S_0 to +1.150 T_1 for complex **2**). This clearly indicates that the excited state has little, if any, MLCT character. The overall charge on the two ligands however does change. The cyclometalating ligand drops in negative charge (e.g., −0.350 in S_0 to −0.142 in T_1 for complex **2**) while for the terpyridine an opposite effect is found (+0.258 in S_0 to +0.009 in T_1 for complex **2**), indicating a net transfer of electron density (ca. 0.25) from the cyclometalated ligand to the terpyridine.

The partial dppy → tpy LLCT character obtained from the DFT calculations agrees well with the conclusions based on experimental data (nanosecond transient absorption and emission spectral shifts accompanying terpyridine substitution). The calculations on isomeric species clearly demonstrate the electron donating−withdrawing effects of the axial substituents, with calculated energies of the triplet state corresponding to 680 and 678 nm for **2** and **4**, respectively (to be compared with experimental emission energies of 684 and 679 nm).

The Ir(III) metal atom is expected to bring about strong spin−orbit coupling, and examples of cyclometalated Ir(III) complexes actually exhibit absorption features of sizable intensity at wavelengths slightly shorter than emission, assigned to spin-forbidden transitions. For the same reason, the emission of such species have often high quantum yields and relatively high (typically, 10^5 s^{-1}) radiative rate constants. Here, on the contrary, the emissions have low quantum yields, despite the long lifetimes, and thus small radiative rate constants (e.g, 1.8×10^4 s^{-1} for **1**). Also no absorption bands of appreciable intensity are observed in the wavelength range between the intense spin-allowed bands and the emission. A possible reason for the unusually low oscillator strengths of the transitions connecting T_1 and S_0 may be related to the peculiar properties of the S_1 state, wherefrom T_1 should primarily steal intensity by spin−orbit coupling. Indeed, it has been noticed above that in these axial complexes S_1 has a substantially symmetry forbidden character, with vanishingly small absorption intensity.

Previous literature on other iridium *trans*-cyclometalated complexes indicate that the *trans* nature of the bis-cyclometalation may contribute to the low emission quantum yield through a deligation mechanism.[16] The experimental results rule out deligation as a source of inefficiency in the present cases. First, such a phenomenon is expected to act by shortening of the excited-state lifetime, which is clearly not the case here. Furthermore, the length of the Ir−C bonds is calculated to remain constant on excitation from S_0 to T_1 and no sign of deligation is seen in the time-resolved experiments.

Conclusions

The cyclometalated complexes described in this work represent a new motif in the chemistry of iridium polypyridyl complexes. The asymmetric bis-tridentate ligand arrangement (C∧N∧C)Ir(N∧N∧N) gives the complexes a nice axial geometry and some peculiar properties. In electrochemistry, it has the effect of moving the reductive properties into a more accessible (less negative) region, while leaving the oxidative process in the typical range of common bis-cyclometalated complexes. In terms of excited-state nature, as shown by the computational results, it provides a directional charge-transfer character. This appears to be a unique property of the *trans* arrangement of the cyclometalated carbons. Although considering the net transfer of charge we assign the excited state as appreciably LLCT in character, it should be kept in mind that in many respects these traditional classifications are not strictly applicable to complexes featuring strongly covalent metal−carbon bonds. Further studies into the properties such type of complexes, as well as the exploitation of the axial geometry to produce rodlike binuclear and polynuclear species, are ongoing.

Acknowledgment. Funding by the EC (Grant G5RD-CT-2002-00776, MWFM) and MIUR (Grant FIRB-RBNE-019H9K) is gratefully acknowledged.

Supporting Information Available: ^{1}H NMR and ^{13}C NMR as additional proof of purity and a structure showing the numbering scheme used to assign protons, optimized geometries in Cartesian coordinates and absolute energies plus additional pictures showing the geometrical parameters commented in this paper, and full electrospray mass spectra of all the complexes. This material is available free of charge via the Internet at http://pubs.acs.org.

IC049277G